

Structural and magnetic studies of *A* site doped $\text{LaRh}_{1-x}\text{Cu}_x\text{O}_3$ ($A = \text{Ca}^{2+}$, Sr^{2+} , Pb^{2+} and Bi^{3+})

Labib Awin^a, Brendan J. Kennedy^{a,*}, Maxim Avdeev^b

^a*School of Chemistry, The University of Sydney, Sydney NSW 2006, Australia*

^b*The Bragg Institute, Australian Nuclear Science and Technology Organization—Private Mail Bag 1, Menai NSW 2234, Australia*

Available online 22 October 2012

Abstract

A site doped Rh perovskites with general formula $\text{La}_{0.75}\text{A}_{0.25}\text{Rh}_{0.7}\text{Cu}_{0.3}\text{O}_3$ and $\text{La}_{0.75}\text{A}_{0.25}\text{Rh}_{0.5}\text{Cu}_{0.5}\text{O}_3$ ($A = \text{Ca}^{2+}$, Sr^{2+} , Pb^{2+} and Bi^{3+}) were synthesized by solid-state methods and their crystallographic, magnetic, and electric properties investigated. Doping by divalent cations resulted in much lower cell volumes and octahedral distortions than doping with a trivalent oxide. The Pb^{2+} and Bi^{3+} ($6s^2$) doped oxides exhibited the lowest magnetic moments and the highest activation energies. Magnetization curves are indicative of antiferromagnetic behavior. The addition of Ca^{2+} , Sr^{2+} , Pb^{2+} and Bi^{3+} cations to the *A*-site decreases the conductivity.

© 2012 Elsevier Ltd and Techna Group S.r.l. All rights reserved.

Keywords: C. Magnetic properties; D. Perovskites; *A*-site doping

1. Introduction

The magnetic properties of many double perovskite oxides remain controversial, and enormous efforts have been deployed searching for improved understanding. One extensively studied system is the alkaline earth *3d-4d* mixed metal perovskites oxides $\text{Sr}_2\text{FeMoO}_6$. The effect of the variation of the *A* site doping on the ferromagnetism is still open to discussion, but it appears that charge delocalization between the *3d* (Fe) and *4d* (Mo) cations is important [1,2].

In the present work, we address the influence of the *A* site doping on the structure, electrical and magnetic properties of some related oxides, $\text{La}_{0.75}\text{A}_{0.25}\text{Rh}_{1-x}\text{Cu}_x\text{O}_3$ where $A = \text{Ca}^{2+}$, Sr^{2+} , Pb^{2+} and Bi^{3+} . The partial substitution at the *A* site is expected to influence the extent of electron delocalization between the two *B* site transition metals similar to that described in $\text{LaRh}_{0.5}\text{Cu}_{0.5}\text{O}_3$ which has $\text{Rh}^{3.5+}$ and $\text{Cu}^{+2.5}$ [3], leading to changes in the physical properties. These changes could be influenced, not only by the differences in the effective charges, but also by differences in the ionic radii and the electron configurations of both the *A* and *B*-site cations. The Pb^{2+} and Bi^{3+} doped oxides are found to exhibit electrical and magnetic behavior different to that of the

alkaline earth doped oxides. This is believed to be a consequence of the stereochemical influence of the $6s^2$ lone pair electrons.

2. Experimental

Commercially available materials La_2O_3 , CuO , Bi_2O_3 , PbO , CaCO_3 and SrCO_3 (Aldrich $\geq 99.9\%$), Rh (Althaca 99.95%) were utilized in the synthesis. The appropriate stoichiometric amounts were mixed, using a mortar and pestle, and then heated in several steps with intermittent regrinding. Samples were initially heated for 24 h at 850 °C followed by reheating at 950 °C for 24 h, and then 1000 °C for 48 h and 1050 °C for 48 h. The samples were finally annealed at 1100 °C for 48 h, until the X-ray diffraction pattern no longer changed.

Neutron powder diffraction data were measured using the high resolution powder diffractometer, Echidna, at the OPAL facility (Australian Nuclear Science and Technology Organization) at a wavelength of 2.4395 Å. Synchrotron X-ray powder diffraction data were collected over the angular range $5 < 2\theta < 85^\circ$, using X-rays of wavelength 0.82554 Å on the powder diffractometer at the Australian Synchrotron.

The magnetic measurements were carried out using a Quantum Design PPMS. The temperature dependence of

*Corresponding author. Tel.: +61 2 9351 2742; fax: +61 2 9351 3329.

E-mail address: B.Kennedy@chem.usyd.edu.au (B.J. Kennedy).

the magnetic susceptibilities was measured under both zero-field cooled (ZFC) and field cooled (FC) conditions in an applied field of 5 kOe over the temperature range 4–300 K. The temperature dependence of the resistivity was measured using a DC four probe technique with the same measurement system.

3. Result and discussion

3.1. Crystal structure

Initially, our synthetic attempts focused on $\text{La}_{0.75}\text{A}_{0.25}\text{Rh}_{0.5}\text{Cu}_{0.5}\text{O}_3$ oxides where $\text{A}=\text{Ca}^{2+}$, Sr^{2+} , Pb^{2+} and Bi^{3+} , however only for Pb^{2+} and Bi^{3+} were single phase samples obtained. Subsequently, the pure members of the series $\text{La}_{0.75}\text{A}_{0.25}\text{Rh}_{0.7}\text{Cu}_{0.3}\text{O}_3$ were prepared. X-ray diffraction measurements showed these are isostructural with undoped LaRhO_3 [4] and have an orthorhombic ($Pbnm$) crystal structure. The structural refinements, from the synchrotron diffraction data, provided precise lattice parameters, however the presence of the very heavy La, Pb and Bi cations limited the accuracy of the refined structures. Consequently, and as illustrated in Fig. 1, neutron diffraction data were also collected for a representative example, $\text{La}_{0.75}\text{Pb}_{0.25}\text{Rh}_{0.5}\text{Cu}_{0.5}\text{O}_3$. The refined structure parameters are given in Table 1. The structural refinement provides no evidence for any anion vacancies. The tilting of the corner sharing MO_6 octahedra for the perovskite $\text{La}_{0.75}\text{Pb}_{0.25}\text{Rh}_{0.5}\text{Cu}_{0.5}\text{O}_3$ ($151.3(3)^\circ$ and $150.16(1)^\circ$) is similar to that reported for LaRhO_3 (150.5° and 149.1°).

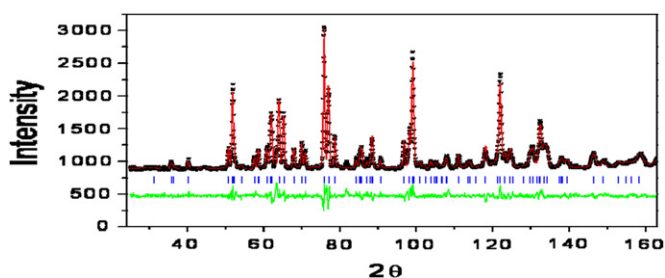


Fig. 1. Neutron diffraction profiles for the $\text{La}_{0.75}\text{Pb}_{0.25}\text{Rh}_{0.5}\text{Cu}_{0.5}\text{O}_3$. The data are represented by the crosses and the solid lines are the calculated and difference profiles. The positions of the space group allowed reflections are shown by the vertical markers immediately below the observed profile.

Table 1

Results of the structural refinements $\text{La}_{0.75}\text{Pb}_{0.25}\text{Rh}_{0.5}\text{Cu}_{0.5}\text{O}_3$ using neutron powder diffraction data. The lattice parameters $a=5.5483(4)$, $b=5.6929(3)$ and $c=7.8447(3)$ Å; The reliability factors $R_p=7.07$, $R_{wp}=9.11$, $\chi^2=2.09$.

Atom	<i>x</i>	<i>y</i>	<i>z</i>	<i>B</i> _{iso} (Å ²)
La/Pb	0.4900 (5)	−0.0499 (4)	0.25	1.66 (10)
Cu/Rh	0	0	0	1.61 (9)
O(1)	0.5875 (6)	0.5222 (6)	0.25	0.85 (13)
O(2)	0.2992 (4)	0.2014 (4)	0.0443 (3)	1.73 (7)

3.2. Unit cell volume

The composition dependence of the unit cell volumes estimated from the synchrotron diffraction data for $\text{La}_{0.75}\text{A}_{0.25}\text{Rh}_{0.7}\text{Cu}_{0.3}\text{O}_3$ and $\text{La}_{0.75}\text{A}_{0.25}\text{Rh}_{0.5}\text{Cu}_{0.5}\text{O}_3$ is illustrated in Fig. 2. Doping with divalent metals, such as Ca and Sr, significantly reduces the cell volume. This is likely driven by the partial oxidation of the Rh^{3+} (6 coordinate ionic radius (IR), 0.67 Å) to Rh^{4+} (0.60 Å) [5] necessary to maintain charge neutrality. Despite the impact of such oxidation, the Pb doped oxide exhibits an increase in the cell volume due to the large ionic size of the Pb^{2+} cation (8 coordinate IR, 1.29 Å). Doping with trivalent metals such as Bi is expected to have little impact on the charge delocalization in the system. The similarity in formal valency of La^{3+} and Bi^{3+} results in no change in the overall charge of the perovskite system. The small increase in cell volume of $\text{La}_{0.75}\text{Bi}_{0.25}\text{Rh}_{0.7}\text{Cu}_{0.3}\text{O}_3$ is consistent with the relative ionic size of the Bi^{3+} (8 coordinate IR, 1.17 Å) and La^{3+} (1.16 Å) cations [5]. The $\text{La}_{0.75}\text{A}_{0.25}\text{Rh}_{0.5}\text{Cu}_{0.5}\text{O}_3$ oxides have lower cell volumes than the corresponding $\text{La}_{0.75}\text{A}_{0.25}\text{Rh}_{0.7}\text{Cu}_{0.3}\text{O}_3$ oxides, presumably due to charge delocalization between the Rh and Cu cations. As described above, partial charge transfer involving Rh^{4+} to Rh^{3+} and Cu^{2+} (6 coordinate IR, 0.73 Å) to Cu^{3+} (0.53 Å) is possible [3]. $\text{La}_{0.75}\text{A}_{0.25}\text{Rh}_{0.5}\text{Cu}_{0.5}\text{O}_3$ has the lowest cell volume in the series, possibly as a consequence of local order effects. It is postulated that both the balance between the long range Coulomb energy and the short range ionic repulsion in the lattice, and A site cation displacements are either modified or enhanced by local ordering or covalency effects of the A site cations resulting in a decrease in the average cell volume [6]. The contraction in the cell volume was seen in the compound $\text{La}_{0.75}\text{A}_{0.25}\text{Rh}_{0.5}\text{Cu}_{0.5}\text{O}_3$ rather than in $\text{La}_{0.75}\text{Bi}_{0.25}\text{Rh}_{0.7}\text{Cu}_{0.3}\text{O}_3$, possibly reflects the solubility limit of Cu ions in the compound with $x=0.5$. It is thought that local clustering of the doped ions is more likely to occur near the solubility limit. It was not possible to prepare single phase samples with $x > 0.5$.

3.3. Octahedral distortion

The diffraction studies demonstrate that both Cu and Rh cations were disordered at the octahedral sites of the perovskite structure. This distortion can be quantified by Eq. (1), where d_i is the individual bond distance between the B site cations and the oxygen anions, and d_{av} is the average of these distances. Δd was estimated to be 1.67×10^{-4} for $\text{La}_{0.75}\text{Pb}_{0.25}\text{Rh}_{0.5}\text{Cu}_{0.5}\text{O}_3$. This value is higher than found for LaRhO_3 ($\Delta d=0.25 \times 10^{-4}$) [7].

$$\Delta d = \sum_i (d_i - d_{av})^2 / (d_{av})^2 \quad (1)$$

Examination of the oxides structures, refined from synchrotron X-ray diffraction data, show that increasing the Cu content from 0.3 to 0.5 significantly increases the

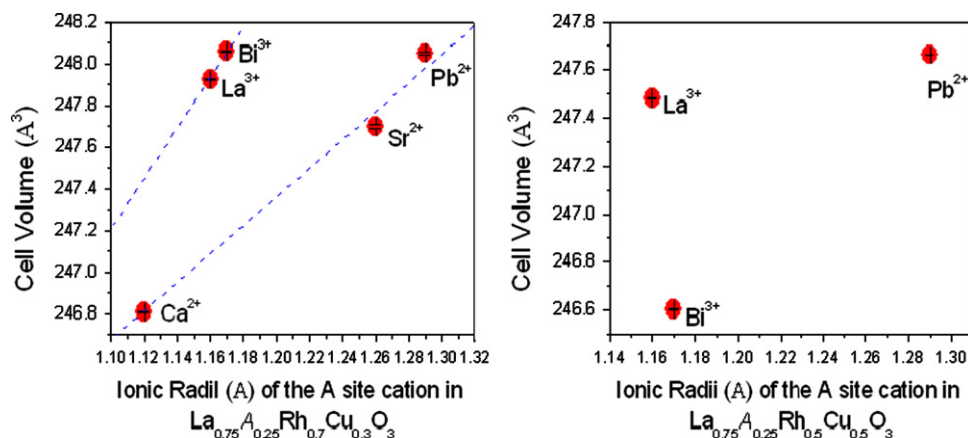


Fig. 2. Composition dependence of the cell volume for $\text{La}_{0.75}\text{A}_{0.25}\text{Rh}_{0.7}\text{Cu}_{0.3}\text{O}_3$ and $\text{La}_{0.75}\text{A}_{0.25}\text{Rh}_{0.5}\text{Cu}_{0.5}\text{O}_3$.

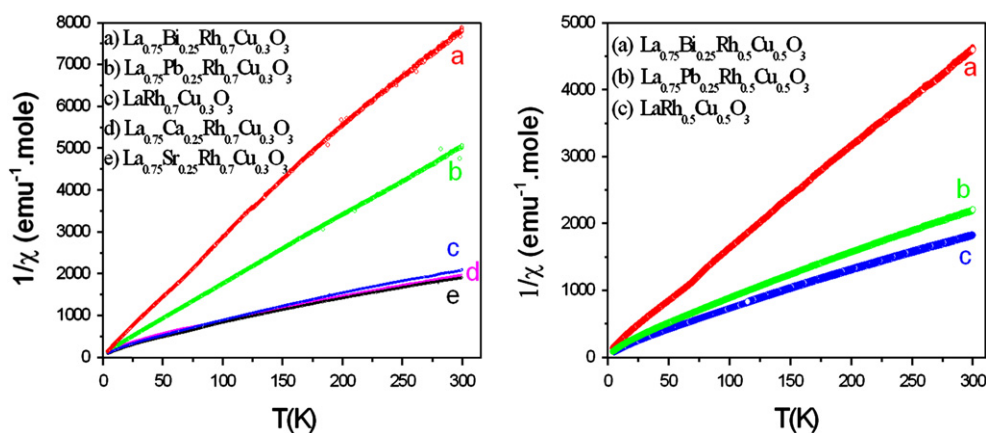


Fig. 3. The temperature dependence of the inverse susceptibility recorded for $\text{La}_{0.75}\text{A}_{0.25}\text{Rh}_{0.7}\text{Cu}_{0.3}\text{O}_3$ and $\text{La}_{0.75}\text{A}_{0.25}\text{Rh}_{0.5}\text{Cu}_{0.5}\text{O}_3$ under zero field cooling conditions with an applied field of 5 T.

octahedral distortion in $\text{La}_{0.75}\text{A}_{0.25}\text{Rh}_{1-x}\text{Cu}_x\text{O}_3$. The octahedral distortion in both $\text{La}_{0.75}\text{Bi}_{0.25}\text{Rh}_{0.5}\text{Cu}_{0.5}\text{O}_3$ (8.76×10^{-4}) and $\text{La}_{0.75}\text{Pb}_{0.25}\text{Rh}_{0.5}\text{Cu}_{0.5}\text{O}_3$ (1.67×10^{-4}) are higher than those in $\text{La}_{0.75}\text{Bi}_{0.25}\text{Rh}_{0.7}\text{Cu}_{0.3}\text{O}_3$ (7.07×10^{-4}) and $\text{La}_{0.75}\text{Pb}_{0.25}\text{Rh}_{0.7}\text{Cu}_{0.3}\text{O}_3$ (0.87×10^{-4}). Surprisingly, Δd is lower in $\text{LaRh}_{0.5}\text{Cu}_{0.5}\text{O}_3$ (2.24×10^{-4}) than in $\text{LaRh}_{0.7}\text{Cu}_{0.3}\text{O}_3$ ($\Delta d = 5.33 \times 10^{-4}$). These changes are believed to result not only from the size effect of the B-site cation (lower tolerance factor), but also from partial oxidation of the Cu^{2+} to Cu^{3+} . The Cu^{2+} ($3d^9$) cations are susceptible to the Jahn–Teller distortion and hence the presence of Cu^{2+} is expected to increase the octahedral distortion. To maintain charge balance, oxidation of Cu^{2+} must be accompanied by reduction of Rh^{4+} to give a mixed valent $\text{Rh}^{3+/4+}$, as observed in $\text{LaRh}_{0.5}\text{Cu}_{0.5}\text{O}_3$ [3]. The differences in the distortion between the various doped samples suggest a shift in the balance of the Cu and Rh redox states. The octahedral distortion is also dependent on the relative sizes of doped cations. For example, the increase in Δd for the perovskite compounds $\text{La}_{0.75}\text{Ca}_{0.25}\text{Rh}_{0.7}\text{Cu}_{0.3}\text{O}_3$ ($\Delta d = 0.65 \times 10^{-4}$) and $\text{La}_{0.75}\text{Sr}_{0.25}\text{Rh}_{0.7}\text{Cu}_{0.3}\text{O}_3$ ($\Delta d = 9.30 \times 10^{-4}$) mimics the change in the (8-coordinate) ionic radii of Ca^{2+} (1.12 Å) and Sr^{2+} (1.26 Å) [5]. This trend is

not seen in the Pb doped oxides; Δd in $\text{La}_{0.75}\text{Pb}_{0.25}\text{Rh}_{0.7}\text{Cu}_{0.3}\text{O}_3$ is lower than in the oxide $\text{La}_{0.75}\text{Sr}_{0.25}\text{Rh}_{0.7}\text{Cu}_{0.3}\text{O}_3$, possibly as a consequence of the stereochemical impact of Pb 6s electrons. There was no obvious correlation found between the octahedral distortion and the M–O(1)–M and M–O(2)–M bond angles in the compounds.

3.4. Magnetization

The inverse susceptibility plots for both series (Fig. 3) demonstrate that in $\text{La}_{0.75}\text{A}_{0.25}\text{Rh}_{0.7}\text{Cu}_{0.3}\text{O}_3$, the susceptibility decreased with doping by Pb and Bi, but increased upon doping with Ca and Sr. Hysteresis loop measurements showed the absence of any long range magnetic ordering in the various oxides. The best linear fits to the inverse magnetization curves showed that the effective magnetic moments (μ_{eff}) for the oxides are negative correlated with Weiss temperatures (θ).

The effective magnetic moments for the Ca^{2+} and Sr^{2+} doped oxides (1.15 and $1.16\mu_B$) are similar to that for $\text{LaRh}_{0.5}\text{Cu}_{0.5}\text{O}_3$ ($1.17\mu_B$), indicating that doping by divalent metals, whether on the A site or B site, has an identical impact on the electron configuration of the transition

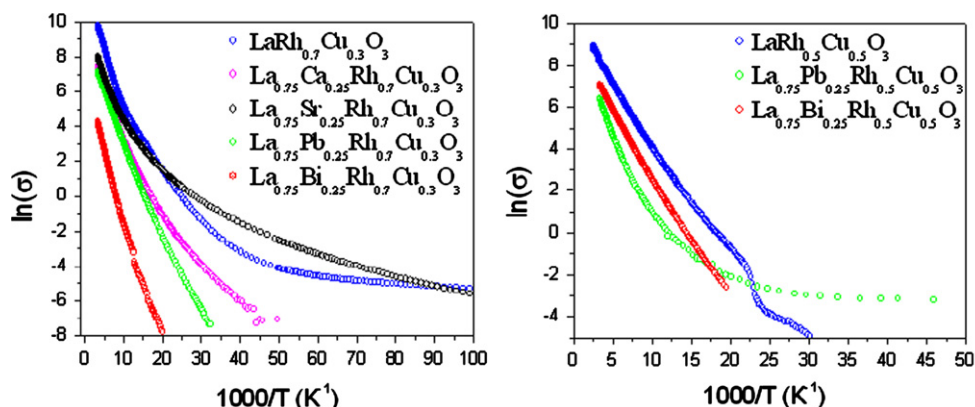


Fig. 4. The Arrhenius plots of $\ln(\sigma)$ for $\text{La}_{0.75}\text{A}_{0.25}\text{Rh}_{0.7}\text{Cu}_{0.3}\text{O}_3$ and $\text{La}_{0.75}\text{A}_{0.25}\text{Rh}_{0.5}\text{Cu}_{0.5}\text{O}_3$ versus inverse temperature.

metals. The increase in inverse magnetic susceptibilities of the doped oxides was consistent with the ranking of electronegativities of the cations ($\text{Sr}^{2+}(0.95) < \text{Ca}^{2+}(1.00) < \text{La}^{3+}(1.10) < \text{Pb}^{2+}(1.87) < \text{Bi}^{3+}(2.02)$) [8]. In the Pb^{2+} and Bi^{3+} doped oxides, the magnetic moments were approximately 30–50% lower than those found for $\text{LaRh}_{0.7}\text{Cu}_{0.3}\text{O}_3$ ($1.11\mu_B$) and $\text{LaRh}_{0.5}\text{Cu}_{0.5}\text{O}_3$. This decrease is not associated with any obvious changes in the M–O(1)–M and M–O(2)–M bond angles, and is thought to be driven, not only by the electronegativity of the cation but also, by the effect of the $6s^2$ lone pair electrons. The Weiss temperature exhibited negative values, lower than seen in the weak paramagnetic oxide LaRhO_3 (-2.74 K , $0.295\mu_B$) [9], indicating the materials are antiferromagnetic.

3.5. Electrical conductivity

Electrical conductivity measurements show that *A*-site doping by either divalent or trivalent metals lowers the conductivity of the perovskites, suggesting an increase in the band gap occurs as a result of the interaction between the valence shell of the *A* site cations and the $3d$ and $4d$ orbitals of the *B* site cations. That was evident from the electrical conductivity (σ) for $\text{LaRh}_{0.7}\text{Cu}_{0.3}\text{O}_3$ ($17.24 \times 10^3\text{ S m}^{-1}$) which is ~ 5 – 20 times higher than those estimated for the Ca, Sr, Pb and Bi doped oxides at 300 K (1.75 , 3.08 , 1.22 and $0.75 \times 10^3\text{ S m}^{-1}$). Also $\sigma_{300\text{ K}}$ for $\text{LaRh}_{0.5}\text{Cu}_{0.5}\text{O}_3$ ($4.35 \times 10^3\text{ S m}^{-1}$) was much higher than $\text{La}_{0.75}\text{Pb}_{0.25}\text{Rh}_{0.5}\text{Cu}_{0.5}\text{O}_3$ ($0.59 \times 10^3\text{ S m}^{-1}$) and $\text{La}_{0.75}\text{Bi}_{0.25}\text{Rh}_{0.5}\text{Cu}_{0.5}\text{O}_3$ ($1.16 \times 10^3\text{ S m}^{-1}$). The Arrhenius plot in Fig. 4 gave an activation energy for $\text{LaRh}_{0.5}\text{Cu}_{0.5}\text{O}_3$ (0.049 eV) that is in good agreement with reported values (0.055 eV) [3], the small difference can be attributed to the different heating regime used to prepare the samples. We find doping with Pb^{2+} and Bi^{3+} results in a small increase in the activation energy from 0.049 eV to 0.065 and 0.055 eV respectively. Likewise in $\text{La}_{0.75}\text{A}_{0.25}\text{Rh}_{0.7}\text{Cu}_{0.3}\text{O}_3$, the activation energies slightly increased from 0.040 eV for $\text{LaRh}_{0.7}\text{Cu}_{0.3}\text{O}_3$ to 0.047 and 0.067 eV for Pb and Bi doped oxides, but decreased to 0.035 and 0.033 eV for Ca and Sr doped oxides respectively. The activation energies of the oxides, in general, are at the range of (0.007 – 0.06 eV) for $\text{La}_{0.75}\text{Sr}_{0.25}\text{RhO}_3$ and

LaRhO_3 respectively [10], suggesting the materials are *p* type semiconductors. The increase in the activation energy of the oxides is consistent with the electronegativity of the *A* site cations (increasing the covalency).

4. Conclusion

The impact of the *A* site doping on the perovskites $\text{La}_{0.75}\text{A}_{0.25}\text{Rh}_{0.7}\text{Cu}_{0.3}\text{O}_3$ and $\text{La}_{0.75}\text{A}_{0.25}\text{Rh}_{0.5}\text{Cu}_{0.5}\text{O}_3$ has been investigated. Differences in the unit cell volumes, structural distortions and magnetization are attributed mainly to the effect of the charge delocalization between the Rh and Cu cations. The trivalent doped oxides display higher cell volumes and octahedral distortions but lower magnetic moments than the divalent oxides. In general, the observed changes in the unit cell volume and the octahedral distortion are consistent with the increase in the ionic radii, whereas the decrease in magnetic moments is correlated with the increase in the electronegativities. One exception is $\text{La}_{0.75}\text{Bi}_{0.25}\text{Rh}_{0.5}\text{Cu}_{0.5}\text{O}_3$ where the contraction in the unit cell volume of is likely related to local ordering effects. The electron configuration influences the spin coupling and the band gap. This is most evident in the Pb^{2+} and Bi^{3+} ($6s^2$) doped oxides which exhibited the lowest magnetic moments and the highest activation energies among the series. Magnetization measurements show the materials are antiferromagnetic where the electrical measurements demonstrate that *A* site doping decreases the conductivity of the oxides.

Acknowledgments

We thank Jimmy Ting for advice on the synthesis. BJK acknowledges the support of the Australian Research Council for this work, and the Australian Synchrotron for provision of beamtime.

References

- [1] R.S. Liu, T.S. Chan, S. Mylswamy, G.Y. Guo, J.M. Chen, J.P. Attfield, Band overlap via chemical pressure control in double perovskite $(\text{Sr}_{2-x}\text{Ca}_x)\text{FeMoO}_6$ with TMR effect, *Current Applied Physics* 8 (2008) 110–113.

- [2] M. García-Hernández, J.L. Martínez, M.J. Martínez-Lope, M.T. Casais, J.A. Alonso, Finding universal correlations between cationic disorder and low field magnetoresistance in FeMo double perovskite series, *Physical Review Letters* 86 (2001) 2443–2446.
- [3] J. Ting, B.J. Kennedy, Z. Zhang, M. Avdeev, B. Johannessen, L.Y. Jang, Synthesis and structural studies of the transition-metal-doped Rh perovskites $\text{LaMn}_{0.5}\text{Rh}_{0.5}\text{O}_3$ and $\text{LaCu}_{0.5}\text{Rh}_{0.5}\text{O}_3$, *Chemistry of Materials* 22 (2010) 1640–1646.
- [4] A. Wold, R.J. Arnott, W.J. Croft, The reaction of rare earth oxides with a high temperature form of rhodium (III) oxide, *Inorganic Chemistry* 2 (1963) 972–974.
- [5] R.D. Shannon, Revised effective ionic-radii and systematic studies of interatomic distances in halides and chalcogenides, *Acta Crystallographica A* 32 (1976) 751–767.
- [6] S. Takagi, A. Subedi, V.R. Cooper, D.J. Singh, Effect of A-site size difference on polar behavior in MBiScNbO_6 ($M=\text{Na, K, and Rb}$): density functional calculations, *Physical Review B* 82 (2010) 134108.
- [7] R.B. Macquart, M.D. Smith, H.C. zur Loye, Crystal growth and single-crystal structures of RERhO_3 ($\text{RE}=\text{La, Pr, Nd, Sm, Eu, Tb}$) orthorhodites from a K_2CO_3 flux, *Crystal Growth and Design* 6 (2006) 1361–1365.
- [8] A.L. Allred, Electronegativity values from thermochemical data, *Journal of Inorganic and Nuclear Chemistry* 17 (1961) 215–221.
- [9] T. Taniguchi, W. Iizuka, Y. Nagata, T. Uchida, H. Samata, Magnetic properties of RRhO_3 ($\text{R}=\text{rare earth}$), *Journal of Alloys and Compounds* 350 (2003) 24–29.
- [10] T.A. Mary, U.V. Varadaraju, Orthorhombic-tetragonal and semiconductor-metal transitions in the $\text{La}_{1-x}\text{Sr}_x\text{RhO}_3$ system, *Journal of Solid State Chemistry* 110 (1994) 176–179.